Advances in the Theory of Nonlinear Analysis and its Applications 7 (2023) No. 4, 130-147.
https://doi.org/10.17762/atnaa.v7.i4.289
Available online at www.https://atnaea.org/
Research Article

Advances in the Theory of Nonlinear Analysis and its Applications

ISSN: 2587-2648 Peer-Reviewed Scientific Journal

Properties of Capturing of Peristaltic Flow to A Chemically Reacting Couple Stress Fluid Through an Inclined Asymmetric Channel with Variable Viscosity and Various Boundaries

Alaa Waleed Salih[a], Ahmed M. Abdulhadi[a]

[a] *Department of Mathematics, College of Science, University of Baghdad, Baghdad, Iraq.*

Abstract

The properties of capturing of peristaltic flow to a chemically reacting couple stress fluid through an inclined asymmetric channel with variable viscosity and various boundaries are investigated. we have addressed the impacts of variable viscosity, different wave forms, porous medium, heat and mass transfer for peristaltic transport of hydro magnetic couple stress liquid in inclined asymmetric channel with different boundaries. Moreover, The Fluid viscosity assumed to vary as an exponential function of temperature. Effects of almost flow parameters are studied analytically and computed. An rising in the temperature and concentration profiles return to heat and mass transfer Biot numbers. Noteworthy, the Soret and Dufour number effect result on temperature and concentration profiles respectively. An incompressible couple stress fluid occupies the porous medium. Stream function that appear under closed form as well as pressure gradient, temperature and the equation of concentration. In a variety of involved parameters, the results are developed. Mathematical analysis is prefer through large wavelength and low Reynolds number. Additionally, the numerical integration is the technique that used to calculate the concentration, velocity, pressure and temperature profiles respectively. Finally, Via using "MATHEMATICA" software we obtain the explanation of physical Zparameters that graphically by a series of figures when apply variety of wave shape.

Keywords: Couple stress fluid; Variable viscosity; Peristaltic flow ; Various boundaries; Porous medium; Inclined asymmetric channel .
2010 MSC: 60G10

Email address: alaa.w@sc.uobaghdad.edu.i (Ahmed M. Abdulhadi)

Received September 22, 2023; Accepted: November 28, 2023; Online: December 22, 2023.

1. Introduction

Nowadays, physiological transport of peristaltic for fluids is an essential method in some instances. Peristaltic motion that shown widely in different applications of engineering, industrial and biological regulation. In human body, flow of blood in small vessels and flow with transport of food bolus as a example about this mechanism of biological fluids. The tube pumps, open heart surgery and hose, etc. are example for helping to explain peristaltic mechanics. In [1] Sohail at el. deal with effects of variable viscosity on the behavior of pressure drop . The peristaltic transport with slip partial that shown by Latha et al. [2] .Some important studies [3, 4, 5, 6] discussed the peristalsis flow. G.S.Seth et al. [7] presented a mathematical frame work for the flow of peristaltic under porous channel. A chemical reaction and flow with slip influences was deal out by Farooq et al. [8]. Muthuraj et al. [9] explored the impact of reaction chemically on hyderomagnetic with dusty fluid in a channel. Non-Newtonian fluid mechanics explain through [10, 11, 12, 13]. In most of other research works deal with the context of non-Newtonian liquid flow are topics between researchers nowadays due to in Refs.[14, 15, 16]. Ramesh [17] studied process of heat and mass transfer in the flow of peristaltic of couple stress fluid in an inclined asymmetric channel trough porous medium . Almost study Ghazi et al. [18] deals with MHD problems under different looks . At Ref. [19] research deal with the impacts of heat and mass transfer on inclined (MHD)peristaltic of pseudo plastic Nano fluid through porous . Effects of porous Medium with variable viscosity on flow of peristaltic in asymmetric channel are discussed via Refs.[20, 21, 22]. Non – Newtonian fluid can't be display with non-slip boundary conditions. In modern days, Almost studies that deal with different form of wave and various boundaries. Analysis of heating influences and different wave forms on peristaltic presented by Akram et al. [23]. The investigation of asymmetric channel on tangent peristaltic flow with porous medium, magnetic field, and heat transfer in wave frame studied by Refs. [24, 25, 26]. Moreover ,Couple stress fluid refers to a specific type of non-Newtonian fluid in which the size of the fluid's particles is taken into consideration. Recent research in this line on couple stress fluid has been considered via various researchers, Eldabe et al.[27] examined peristalsis motion of Eyring-Powell fluid with couple stress and heat and mass transfer under the effect of magnetic field. Almost research in Refs. [28, 29, 30] has been conducted the analysis of couple stress and temperature through different boundary conditions. Mechanism of MHD flow and heat transfer was described by Manjunatha et al.[31]. For more details and more applications , we share in this studies the reader to [32, 33, 34, 35, 36, 37, 38] to show effect of analysis for variable viscous through peristaltic tube or channel. In addition, Disu et al. [39] the authors considered a porous medium between two vertical wavy with viscosity model. Foe instance, the influence of gyrotactic microorganisms over a nonlinear stretching sheet with variable viscosity using HAM discussed via Ref [40].

Different form of boundary duo to notable studies that effect on hydromagnetic peristaltic flow of non-Newtonian fluid where it has now become one of the leading topics between researchers in this days. Various wave forms of peristaltic transport of non-Newtonian fluid described via Hariharan et al. [41]. Nadeem et al. [42] unfolded peristaltic flow of a Maxwell model through porous boundaries. In [43], Adnan et al. explain the influence of an inclined magnetic field on peristaltic flow of Bingham plastic fluid in an inclined symmetric channel. Applications of extended simple equation method on unstable nonlinear Schrödinger equations proposed by Lu et al. [44]. Some other outstanding research works in context of flow with non-Newtonian liquid duo to Refs. [45, 46, 47, 48]. Akram et al. [49, 50] depicted the remarkable research on heating impacts and different wave forms on peristaltic flow of fluid.

The aim focus in this review has been to analysis fluid flow of peristalsis in an inclined tube as well as porous medium existing. Through a quick look at the changes that have been represented by graphs. This research is designed to determine and explain the effects of magnetic field, Hartmann number, porosity parameter and various boundaries on temperature, axial velocity, concentration, pressure gradient profiles respectively. At first, pointed equations for the fluid are significant, Then the mathematically result is solved below a large wavelength and little Reynolds number approximation. Finally, graph of all results that shown to present the physical manner of different emerging parameters has been considered and presented.

2. Formulation of the problem

Let us consider MHD peristaltic transport of non-Newtonian incompressible couple stress fluid in a two-dimensional channel of width $d_1 + d_2$ is taken into account. Asymmetry of the channel that choose constant speed (c) along the walls with various amplitudes and phases. (α) is the inclination angle of the channel.

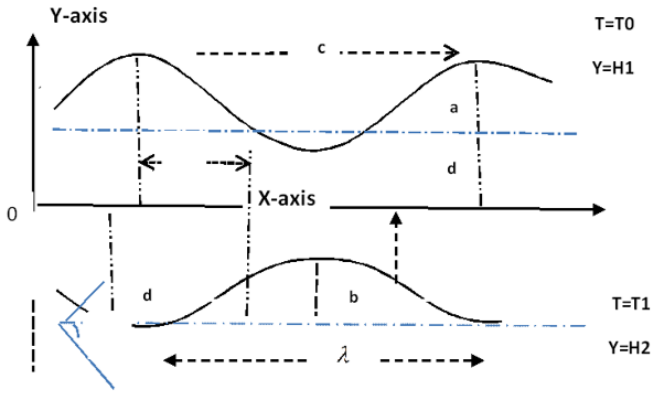

Figure 1: Geometry of problem

3. Expressions for distinct wave types

The investigation deals with peristaltic transport when taken various types of wave shapes that can be taken into account for it. The boundary wall equation are as follows [7] :

1. Trapezoidal waves

$$h_1(x) = 1 + a\left[\frac{32}{\pi^2}\sum_{m=1}^{\infty}\frac{\sin\left(\frac{\pi}{8}(2m-1)\right)}{(2m-1)^2}\sin\left(2\pi(2m-1)x\right)\right] \tag{1}$$

$$h_2(x) = -d - b\left[\frac{32}{\pi^2}\sum_{m=1}^{\infty}\frac{\sin\left(\frac{\pi}{8}(2m-1)\right)}{(2m-1)^2}\sin\left(2\pi(2m-1)x + \phi\right)\right] \tag{2}$$

2. Square waves

$$h_1(x) = 1 + a\left[\frac{4}{\pi}\sum_{m=1}^{\infty}\frac{(-1)^{n+1}}{2n-1}\cos\left(2\pi(2m-1)x\right)\right] \tag{3}$$

$$h_2(x) = -d - b\left[\frac{4}{\pi}\sum_{m=1}^{\infty}\frac{(-1)^{n+1}}{2n-1}\cos\left(2\pi(2m-1)x + \phi\right)\right] \tag{4}$$

4. The governing equations

The fundamental governing flow equations of motion in the present investigation for Non-Newtonian fluid model with couple stress through an inclined asymmetric tapered channel for the current problem are given by [7]:

The Continuity equation representing by:

$$\frac{\partial U}{\partial x} + \frac{\partial V}{\partial y} = 0, \tag{5}$$

The Momentum equations representing by:

$$\rho\left(\frac{\partial U}{\partial t}+U\frac{\partial U}{\partial x}+V\frac{\partial U}{\partial y}\right)=-\frac{\partial P}{\partial x}+\bar{\mu}\left(T\right)\left(\frac{\partial^2 U}{\partial x^2}+\frac{\partial^2 U}{\partial y^2}\right)-\eta\left(\frac{\partial^4 U}{\partial x^4}+2\frac{\partial^4 U}{\partial x^2\partial y^2}+\frac{\partial^4 U}{\partial y^4}\right)$$
$$-\sigma B_o^2\cos\emptyset\left[U\cos\emptyset-V\sin\emptyset\right]-\frac{\bar{\mu}\left(T\right)}{k_o}U+\rho g\sin\alpha, \tag{6}$$

$$\rho\left(\frac{\partial V}{\partial t}+U\frac{\partial V}{\partial x}+V\frac{\partial V}{\partial y}\right)=-\frac{\partial P}{\partial y}+\bar{\mu}\left(T\right)\left(\frac{\partial^2 V}{\partial x^2}+\frac{\partial^2 V}{\partial y^2}\right)-\eta\left(\frac{\partial^4 V}{\partial x^4}+2\frac{\partial^4 V}{\partial x^2\partial y^2}+\frac{\partial^4 V}{\partial y^4}\right)$$
$$-\sigma B_o^2\cos\emptyset\left[U\cos\emptyset-V\sin\emptyset\right]-\frac{\bar{\mu}\left(T\right)}{k_o}V+\rho g\sin\alpha, \tag{7}$$

$$\rho c_p\left(\frac{\partial T}{\partial t}+U\frac{\partial T}{\partial x}+V\frac{\partial T}{\partial y}\right)=k\left(\frac{\partial^2 T}{\partial x^2}+\frac{\partial^2 T}{\partial y^2}\right)+2\bar{\mu}\left(T\right)\left[\left(\frac{\partial U}{\partial x^2}\right)^2+\left(\frac{\partial V}{\partial y^2}\right)^2\right]+\bar{\mu}\left(T\right)\left(\frac{\partial U}{\partial y}+\frac{\partial V}{\partial x}\right)^2$$
$$+\eta\left[\left(\frac{\partial^2 U}{\partial x^2}+\frac{\partial^2 U}{\partial y^2}\right)^2+\left(\frac{\partial^2 V}{\partial x^2}+\frac{\partial^2 V}{\partial y^2}\right)^2\right]+D\frac{k_T}{c_s}\left(\frac{\partial^2 C}{\partial x^2}+\frac{\partial^2 C}{\partial y^2}\right)+Q_o \tag{8}$$

$$\frac{\partial C}{\partial t}+U\frac{\partial C}{\partial x}+V\frac{\partial C}{\partial y}=D\left(\frac{\partial^2 C}{\partial y^2}+\frac{\partial^2 C}{\partial x^2}\right)+D\frac{k_T}{T_m}\left(\frac{\partial^2 T}{\partial y^2}+\frac{\partial^2 T}{\partial x^2}\right)-k_1\left(C-C_o\right), \tag{9}$$

As $U(x,y,t)$ and $V\left(x,y,t\right)$ refer to the components of velocity along x-direction and y- direction respectively.

Here $\{P,T,\rho,\mu,B_o,\sigma,\emptyset,\alpha,D,C,\eta\ ,k,k_T,T_m,c_s,c_p,g,k_1,k_o,Q_o\}$ designate the pressure, the temperature, fluid density, dynamic viscosity, magnetic strength, electrical conductivity, the inclination angle of vertical axis, an inclination angle to horizontal axis, coefficient of mass diffusivity, the concentration, couple stress fluid viscosity parameter, thermal conductivity, thermal diffusion ratio, temperature of medium, concentration susceptibility, specific heat, gravitational acceleration , chemical reaction parameter, permeability parameter ,and heat generation parameter respectively.

However, the relationship between the two frames is displayed for stable flow by the following form and it can be treated as steady flow in a coordinate system $(\overline{x},\overline{y})$, where we switch form laboratory frame to wave frame as follows

$$x=X-ct, y=Y, v=V, u=U-c, p=P \tag{10}$$

In which the velocity components, pressure temperature and concentration in the wave frame is designated respectively by u,v,p,T,C .

Although, to generalize the above system of Eqs. (6-9), the non-dimensional variables and quantities encountered in our analysis can be written as [7] :

$$\left.\begin{aligned}
&u=\frac{\bar{u}}{c},v=\frac{\bar{v}}{c},x=\frac{\bar{x}}{\lambda},y=\frac{\bar{y}}{d_1},p=\frac{\bar{p}\lambda\mu_0 c}{d_1^2},\delta=\frac{d_1}{\lambda},t=\frac{\bar{t}\lambda}{c},\\
&R_e=\frac{\rho d_1 c}{\mu_0},\ M=\sqrt{\frac{\sigma}{\mu_0}}B_0 d_1,F_r=\frac{c^2}{gd_1},\ P_r=\frac{\mu_0 c_p}{k},D_a=\frac{k_0}{d_1^2},\gamma^2=\frac{\mu_0}{\eta}d_1^2\\
&E_c=\frac{c^2}{c_p\left(\Delta T\right)},S_c=\frac{\mu_0}{\rho D},S_r=\frac{\rho D k_T\left(\Delta T\right)}{\mu_0\left(\Delta C\right)},\sigma=\frac{C-C_0}{\left(\Delta C\right)},\theta=\frac{T-T_0}{\left(\Delta T\right)},\gamma_1=\frac{k_1 d_1^2\rho}{\mu_0}\\
&\beta=\frac{Q_o d_1^2}{k\left(\Delta T\right)},B_m=\frac{h_m d_1}{k_m},B_h=\frac{h_h d_1}{k_h},D_u=\frac{Dk_T\left(\Delta C\right)}{\mu_0 c_s c_p\left(\Delta T\right)},\mu\left(\theta\right)=\frac{\mu\left(T\right)}{\mu_0}
\end{aligned}\right\} \tag{11}$$

Which, in term of stream function (ψ) , the components velocity with dimensionless are represent below by that :

$$u=\frac{\partial\psi}{\partial y},v=-\delta\frac{\partial\psi}{\partial x} \tag{12}$$

Where $\delta, R_e, M, F_r, P_r, D_a, \gamma, \gamma_1, E_c, S_c, S_r, \sigma, \theta, D_u, B_h\ , B_m, \beta, \Delta T = T_1 - T_0$ and ψ are as follows, The wave number ,Reynolds number, Hartman number, Froude number, Prandtl number, Darcy number, parameter of couple stress fluid, parameter of chemical, Eckert number, Schmidt number, Sort number, dimensionless concentration, dimensionless temperature, Dufour number, heat mass transfer, Biot number, parameter of source/sink heat generation, T_1 temperature at h_2, T_0 temperature at h_1 and stream function respectively.

If we incorporate variables of Eq.(11) into Eqs.(6-9), then we getting the following formulas :

$$\begin{aligned} R_e\ \delta\frac{\partial u}{\partial t} + R_e\delta u\frac{\partial u}{\partial x} + R_e\ v\frac{\partial u}{\partial y} =& -\frac{\partial p}{\partial x} + \mu(\theta)\left(\delta^2\frac{\partial^2 u}{\partial x^2} + \frac{\partial^2 u}{\partial y^2}\right) - \frac{1}{\gamma^2}\delta^4\frac{\partial^4 u}{\partial x^4} \\ & - \frac{1}{\gamma^2}\frac{\partial^4 u}{\partial y^4} - 2\frac{1}{\gamma^2}\delta^2\frac{\partial^4 u}{\partial x^2\partial y^2} - M^2\cos\emptyset\left[(u+1)\cos\emptyset - v\sin\emptyset\right] \\ & - \frac{1}{D_a}\mu(\theta)(u+1) + \frac{\rho d_1 c}{\mu_o}\cdot\frac{g d_1}{c^2}\sin\alpha \end{aligned} \tag{13}$$

$$\begin{aligned} R_e\delta^2\ u\frac{\partial v}{\partial x} + R_e\delta\ v\frac{\partial v}{\partial y} =& -\frac{\partial p}{\partial y} + \mu(\theta)\left(\frac{\partial^2 v}{\partial y^2} + \delta^{\ 3}\frac{\partial^2 v}{\partial x^2}\right) - \frac{1}{\gamma^2}\delta^4\frac{\partial^4 v}{\partial x^4} \\ & - \frac{1}{\gamma^2}\delta\frac{\partial^4 v}{\partial y^4} - 2\frac{1}{\gamma^2}\delta^3\frac{\partial^4 v}{\partial x^2\partial y^2} - M^2\delta\cos\emptyset\left[(u+1)\cos\emptyset - v\sin\emptyset\right] \\ & - \frac{1}{D_a}\mu(\theta)\delta v - \delta\frac{\rho d_1 c}{\mu_o}\cdot\frac{g d_1}{c^2}\sin\alpha \end{aligned} \tag{14}$$

$$\begin{aligned} R_e P_r\delta\left(u\frac{\partial\theta}{\partial x} + v\frac{\partial\theta}{\partial y}\right) =& \left(\delta^2\frac{\partial^2\theta}{\partial x^2} + \frac{\partial^2\theta}{\partial y^2}\right) + \mu(\theta)P_r E_c\ (\ 2\delta^2\left(\frac{\partial u}{\partial x}\right)^2 + 2\left(\frac{\partial v}{\partial y}\right)^2 + \left(\frac{\partial u}{\partial y} + \delta\frac{\partial v}{\partial x}\right)^2 + \\ & \frac{1}{\gamma^2}\left[\left(\delta^2\frac{\partial^2 u}{\partial x^2} + \frac{\partial^2 u}{\partial y^2}\right)^2 + \left(\delta^2\frac{\partial^2 v}{\partial x^2} + \frac{\partial^2 v}{\partial y^2}\right)^2\right]) + D_u P_r\left(\delta^2\frac{\partial^2\sigma}{\partial x^2} + \frac{\partial^2\sigma}{\partial y^2}\right) + \beta \end{aligned} \tag{15}$$

$$R_e\delta\left(u\frac{\partial\sigma}{\partial x} + \frac{1}{\delta}v\frac{\partial\sigma}{\partial y}\right) = \frac{1}{S_c}\left(\delta^2\frac{\partial^2\sigma}{\partial x^2} + \frac{\partial^2\sigma}{\partial y^2}\right) + S_r\left(\delta^2\frac{\partial^2\theta}{\partial x^2} + \frac{\partial^2\theta}{\partial y^2}\right) - \gamma_1\sigma \tag{16}$$

Now, via using long wavelength approximation δ $(\delta \ll 1)$, with considering low Reynolds number $(R_e \to 0)$ and relationship in Eq.(12), Then, the Eqs. (13–16) become as below.

$$\frac{\partial\psi}{\partial x\partial y} - \frac{\partial\psi}{\partial y\partial x} = 0, \tag{17}$$

$$\frac{\partial p}{\partial x} = \mu(\theta)\left(\frac{\partial^3\psi}{\partial y^3}\right) - \frac{1}{\gamma^2}\left(\frac{\partial^5\psi}{\partial y^5}\right) - \left[M^2 cos^2\emptyset + \frac{1}{D_a}\mu(\theta)\right]\left(\frac{\partial\psi}{\partial y} + 1\right) - M^2\delta\frac{\partial\psi}{\partial x}\cos\emptyset\sin\emptyset + \frac{R_e}{F_r}\sin\alpha, \tag{18}$$

$$\frac{\partial p}{\partial y} = 0, \tag{19}$$

$$\frac{\partial^2\theta}{\partial y^2} + \mu(\theta)B_r\left[\left(\frac{\partial^2\psi}{\partial y^2}\right)^2 + \frac{1}{\gamma^2}\left(\frac{\partial^3\psi}{\partial y^3}\right)^2\right] + D_u P_r\frac{\partial^2\sigma}{\partial y^2} + \beta = 0, \tag{20}$$

$$\frac{\partial^2\sigma}{\partial y^2} + S_r S_c\frac{\partial^2\theta}{\partial y^2} - S_c\gamma_1\sigma = 0, \tag{21}$$

Although, via eliminating of pressure from Eq.(18) leads to

$$\mu(\theta)\left(\frac{\partial^4\psi}{\partial y^4}\right) - \frac{1}{\gamma^2}\left(\frac{\partial^6\psi}{\partial y^6}\right) - \left[M^2 cos^2\emptyset + \frac{1}{D_a}\mu(\theta)\right]\frac{\partial^2\psi}{\partial y^2} = 0, \tag{22}$$

For the easily manuscript, most investigations on fluid mechanics take constant viscosity, but in this paper we study variation of viscosity depend on fact of the viscosity is a function of heat, with dimensionless temperature, the following form was proposed by [6].

$$\mu(\theta) = e^{-\epsilon\theta} \text{ or } \mu(\theta) = 1 - \epsilon\theta \text{ where } \epsilon \ll 1. \tag{23}$$

where (ϵ) is the viscosity parameter , which is constant.

By rearrangement Eq.(18) and Eq. (22), the non-dimensional will be

$$\begin{aligned}\frac{\partial p}{\partial x} &= (1-\epsilon\theta)\left(\frac{\partial^3\psi}{\partial y^3}\right) - \frac{1}{\gamma^2}\left(\frac{\partial^5\psi}{\partial y^5}\right) - \left[M^2 cos^2\emptyset + \frac{1}{D_a}(1-\epsilon\theta)\right]\left(\frac{\partial\psi}{\partial y}+1\right) \\ &\quad - M^2\delta\frac{\partial\psi}{\partial x}\cos\emptyset\sin\emptyset + \frac{R_e}{F_r}\sin\alpha,\end{aligned} \tag{24}$$

$$(1-\epsilon\theta)\left(\frac{\partial^4\psi}{\partial y^4}\right) - \frac{1}{\gamma^2}\left(\frac{\partial^6\psi}{\partial y^6}\right) - \left[M^2 cos^2\emptyset + \frac{1}{D_a}(1-\epsilon\theta)\right]\frac{\partial^2\psi}{\partial y^2} = 0\ , \tag{25}$$

The suitable boundary conditions in dimensionless wave frame are at different waves, model-i (Trapezoidal waves) and model-ii (Square waves) as follow

$$\left.\begin{aligned}\psi = \frac{F}{2}, \frac{\partial^3\psi}{\partial y^3} = 0, \frac{\partial\psi}{\partial y} = -1,\ At\ y = h_1 \\ \psi = -\frac{F}{2}, \frac{\partial^3\psi}{\partial y^3} = 0, \frac{\partial\psi}{\partial y} = -1,\ At\ y = h_2\end{aligned}\right\} \tag{26}$$

Also,

$$\left.\begin{aligned}\frac{\partial\theta}{\partial y} = (1-\theta)B_h, \frac{\partial\sigma}{\partial y} = (1-\sigma)B_m,\ At\ y = h_2 \\ \frac{\partial\theta}{\partial y} = (\theta)B_h, \frac{\partial\sigma}{\partial y} = (\sigma)B_m,\ At\ y = h_1\end{aligned}\right\} \tag{27}$$

Expression of the stream function that keeping with subjected boundary conditions Eq.(26), where $\{F\}$ is the non- dimensional mean flow rate in the wave frame:

$$\psi = 2[\frac{e^{k_4 y}}{k_6}c_1 + \frac{e^{-k_4 y}}{k_6}c_2 + \frac{e^{k_5 y}}{k_7}c_3 + \frac{e^{-k_5 y}}{k_7}c_4 + c_5 + yc_6, \tag{28}$$

$$\left.\begin{aligned}k_4 = \sqrt{\frac{\frac{1-\sqrt{1-4a_1(a_2+a_3)}}{a_1}}{2}}, k_5 = \sqrt{\frac{\frac{1+\sqrt{1-4a_1(a_2+a_3)}}{a_1}}{2}} \\ k_6 = \frac{1-\sqrt{1-4a_1(a_2+a_3)}}{a_1}, k_7 = \frac{1+\sqrt{1-4a_1(a_2+a_3)}}{a_1}\end{aligned}\right\} \tag{29}$$

The values of coefficients $\{c_1, c_2, c_3, c_4, c_5, c_6\}$ are so large, then their quantities be calculate under boundary conditions Eq.(26) via using Mathematica program .

Then, we obtain the exact solution for temperature (θ) Eq. (26), satisfy the boundary conditions (27), as the following term yields.

$$\begin{aligned}\theta =& c_5 + yc_6 + \frac{1}{k_6^2k_7^2\gamma^2}[-\frac{1}{2}k_6^2k_7^2y^2\beta\gamma^2 + 8\left[c_1c_4 - c_2c_3 - c_1c_3 + c_2c_4\right] \\ & e^{-(k_4-k_5)y}k_4^2k_5^2k_7\left(k_4k_5 - \gamma^2\right)\alpha B_r - c_3^2e^{2k_5y}k_5^2\left(k_5^2+\gamma^2\right)\alpha B_r + 4y^2(c_3c_4k_5^6 - c_3c_4k_5^4k_6^2\gamma^2 - c_1c_2k_4^4k_7^2\gamma^2)\alpha B_r \\ & + 2e^{-2(k_4+k_5)y}\left(-\frac{1}{2}c_2^2e^{2k_5y}k_5^2k_6^2\left(k_5^2+\gamma^2\right)\alpha B_r + \frac{1}{-4(k_4+k_5)-p_1}e^{(-4(k_4-k_5)+p_{1)y}}k_6^2k_7^2\left(4(k_1+k_5)+p_1\right)\right. \\ & p_3\big(p_2 - p_3 + p_4 + 8c_4k_4^2k_5^2k_6p_5 - 32c_4k_4^2k_5^2k_6k_8k_{11}p_5 - 23c_4k_4^2k_5^2k_6p_5 + 128c_4k_4^2k_5^2k_6p_6 - 32c_4k_4^2k_5^2k_6k_8k_{11}p_6 \\ & + 128c_4k_4^2k_5^2k_6k_8^2p_6 + 8c_4k_{11}^2k_5^2k_6p_7 - 32c_4k_4^2k_5k_8k_{11}p_7 - 23c_4k_5^2k_6k_{11}k_8p_7 + (p_9+p_{10})\gamma^2D_uP_r\big),\end{aligned} \tag{30}$$

While solution of concentration, substituting equation of temperature as shown in Eq.(**??**) with boundary condition Eq.(27)

$$\begin{aligned}\sigma =&[e^{\left(-(4(k_4-k_5))+\sqrt{\frac{k_{11}}{k_8}}\right)y}[k_{11}k_5^4k_6^2\left(k_4-4k_4^2k_8\right)\left(k_{11}^2-2k_4k_8\left(k_4^2-k_5^2\right)\right)+\left(k_8^2\left(k_4^2-k_5^2\right)\right)\\&\left(k_{10}k_5^2+k_9\right)[4c_4^2e^{\left(4k_4+2k_5+\sqrt{\frac{k_{11}}{k_8}}\right)y}+4c_3^2e^{\left(4k_4+6k_5+\sqrt{\frac{k_{11}}{k_8}}\right)y}]-8c_3k_{11}k_4^2k_5^2k_6k_7(k_{11}-4k_4^2k_8)\\&\left(k_{11}-4k_5^2k_8\right)[c_2e^{\left(3k_4+5k_5+\sqrt{\frac{k_{11}}{k_8}}\right)y}\left(k_{11}-\left(k_4+k_5\right)^2k_8\right)\left(k_{10}k_4k_5-k_9\right)+c_1\\&\left(-k_{11}+\left(k_4-k_5\right)^2k_8\right)\left(k_{10}k_4k_5+k_9\right)]8c_4k_5^2k_6\left(k_{11}-4k_4^2k_8\right)\left(k_{11}-4k_5^2k_8\right)\\&\left[-c_3e^{\left(4k_4+4k_5+\sqrt{\frac{k_{11}}{k_8}}\right)y}k_5^2k_6(k_{11}^2-2k_{11}k_8\left(k_4^2+k_5^2\right)+k_8^2\left(k_4^2-k_5^2\right)\left(k_{10}k_5^2+k_9\right)\right]/(k_{11}k_6^2k_7^2(\sqrt{k_{11}}-2k_4\sqrt{k_8}))\\&2(\sqrt{k_{11}}+2k_4\sqrt{k_8})(\sqrt{k_{11}}+\sqrt{k_8}\left(k_4-k_5\right))(\sqrt{k_{11}}+2k_5\sqrt{k_8})(\sqrt{k_{11}}-2k_5\sqrt{k_8})\\&(\sqrt{k_{11}}+\sqrt{k_8}\left(k_5-k_4\right))(\sqrt{k_{11}}-\sqrt{k_8}\left(k_4+k_5\right))(\sqrt{k_{11}}+\sqrt{k_8}\left(k_4+k_5\right)),\end{aligned} \tag{31}$$

The values of coefficients $(p_1,\ p_2, p_3, p_4, p_5, p_6, p_7, p_8, p_9, p_{10}, p_{11}, k_5, k_6, k_7, k_8, k_9, k_{10}, k_{11})$ are long non-constant and their amounts can be determined with the boundary conditions in Eq.(27) via using program Mathematica 11. In addition, these coefficients can change when we apply different forms of wave shape.

5. Graphical results and discussions

In subsections (5.1 – 5.5), discuss the effects of various parameters and deep analysis on velocity distribution (u), temperature (θ), concentration (σ), pressure gradient (dp/dx) profiles and stream lines with trapping phenomena. In this section, we have presented a set of figures to observe and describe the behavior of various variables. The phenomenon of trapping are also explained for trapezoidal and square waves through plotting. The results are obtain in term of graphs.

5.1. Velocity profile

We calculate in this subsection the axial velocity via using related parameters that impact on profile of it. The change for various values of $(\gamma, M, \emptyset, D)$ are clearly in Figures (1-4). As shown in figures, the velocity profiles taken parabolic shape. Additionally, Figure 1 explain the variation in fluid couple stress parameter (γ) with velocity profile when the decreasing of it return to the increasing in values of this parameter at all wave boundary shape we using. For increasing Hartmann number (M), the velocity decrease within period, also variation of profile that different and expansion at trapezoidal wave as shown in Figure 2. In addition, Figure 3 exhibits distribution of velocity under effect of $(\emptyset)$ for both model and observe decreasing of profile with point of inflexion in the middle. When the value of (D) increased, the axial velocity profile increases at wall channel as we denoted in Figure 4 in both model. Clearly, we noted physical confirmation behind reduction of velocity down the center of the channel. Moreover, the fluid velocity is satisfied boundary condition.

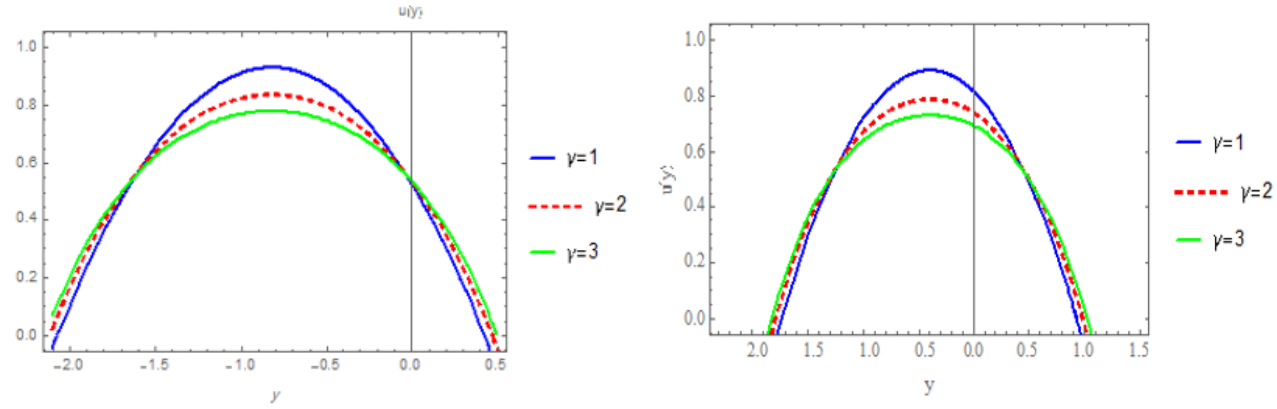

(a) Model-i: Trapezoidal wave (b) Model- ii: Square wave

Figure 2: The variation of axial velocity profile (u) for distinct values (γ), at $M = 1, \emptyset = \frac{\pi}{6}$, $a = 0.5, b = 1, d = 1.8, \epsilon = 0.05, x = 1.2,\ D = 0.8, \alpha = 3$.

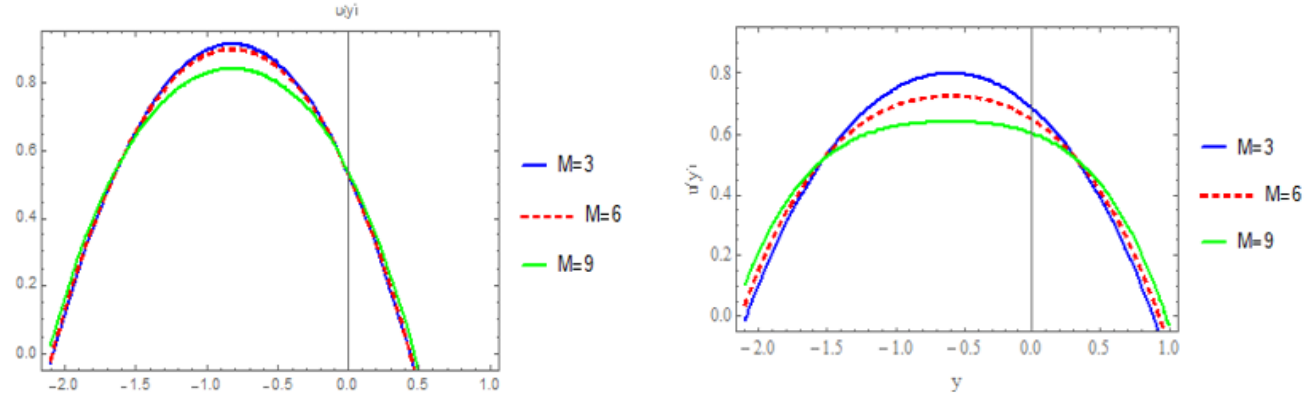

(a) Model-i: Trapezoidal wave (b) Model- ii: Square wave

Figure 3: The variation of axial velocity profile (u) for distinct values of (M) at $\gamma = 1, \emptyset = \frac{\pi}{6}, a = 0.5, b = 1, d = 1.8, \epsilon = 0.05, x = 1.2, D = 0.8, \alpha = 3$.

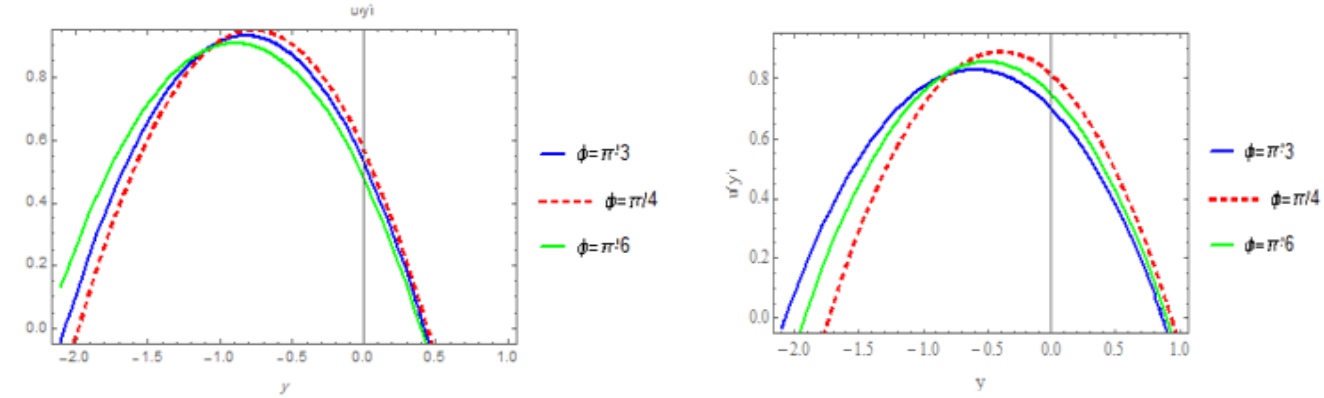

(a) Model-i: Trapezoidal wave (b) Model- ii: Square wave

Figure 4: The variation of axial velocity profile (u) for distinct values of $(\emptyset)$ at $\gamma = 1, M = 1, a = 0.5, b = 1, d = 1.8, \epsilon = 0.05, x = 1.2, D = 0.8, \alpha = 3$.

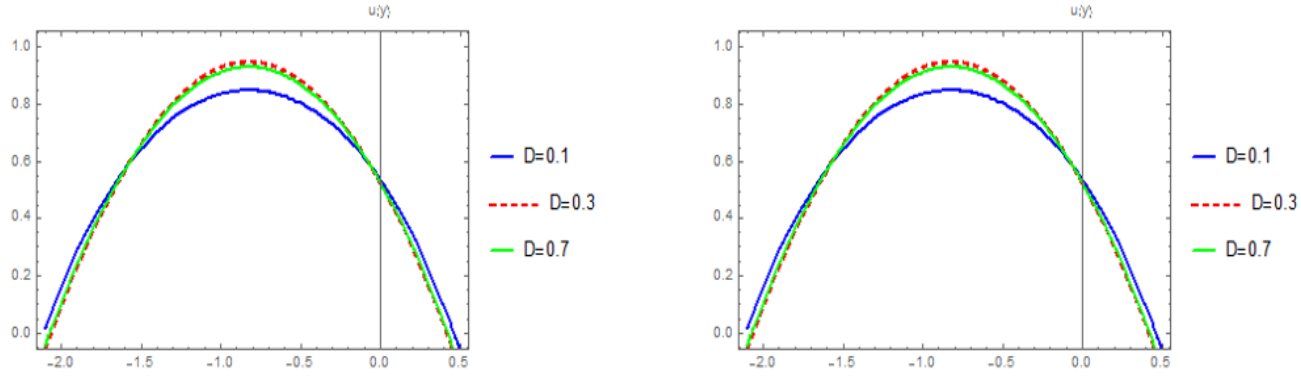

(a) Model-i: Trapezoidal wave (b) Model- ii: Square wave

Figure 5: The variation of axial velocity profile (u) for distinct values of (D) at $\gamma = 1, M = 1, \emptyset = \frac{\pi}{6}, a = 0.5, b = 1, d = 1.8, \epsilon = 0.05, x = 1.2, \alpha = 3$.

5.2. Temperature profile

We have analyze the influences of various flow parameters on the temperature profiles of fluid that explained in Figures (5-8). Figures (5-8) is plotted for various values of $(D_u), (\beta), (\emptyset)$ and (D) on (θ). Denoted that, the temperature profile increases on the inner wall of channel (solid wall). An enhancement in fluid temperature is return to increasing of phase difference.

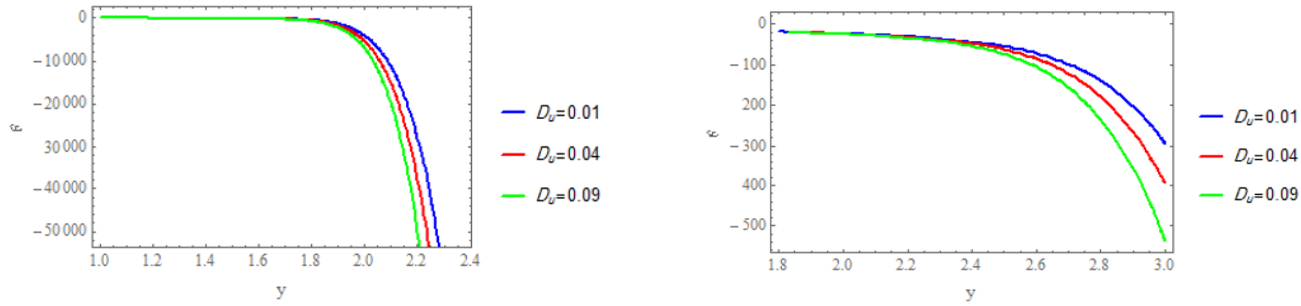

(a) Model-i: Trapezoidal wave (b) Model- ii: Square wave

Figure 6: The variation of Temperature profile (θ) for distinct values of (D_u) at $\gamma = 1, M = 1, \emptyset = \frac{\pi}{4}, a = 0.5, b = 1, \gamma_1 = 0.01, d = 1.8, x = 1.2, \alpha = 3, S_c = 1.5, S_r = 1, P_r = 0.01, \beta = 9, D = 0.03$.

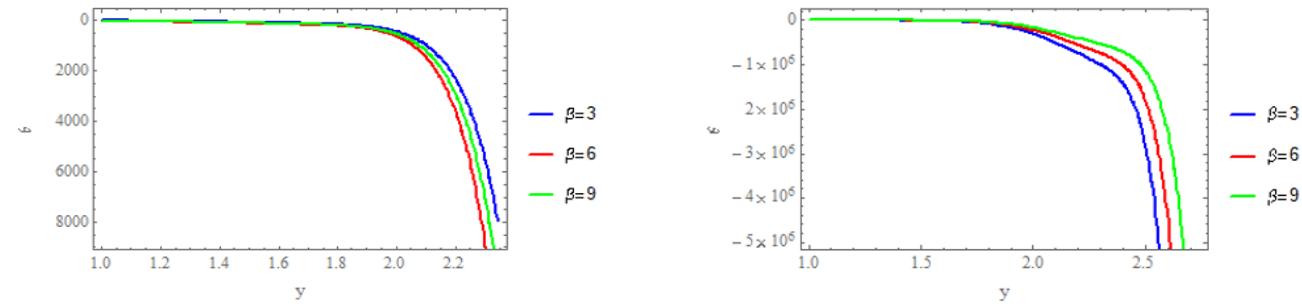

(a) Model-i: Trapezoidal wave (b) Model- ii: Square wave

Figure 7: The variation of Temperature profile (θ) for distinct values of (β) at $\gamma = 1, M = 1, \emptyset = \frac{\pi}{4}, a = 0.5, b = 1, \gamma_1 = 0.01, d = 1.8, x = 1.2, \alpha = 3, S_c = 1.5, S_r = 1, P_r = 0.01, D_u = 0.01, D = 0.03$.

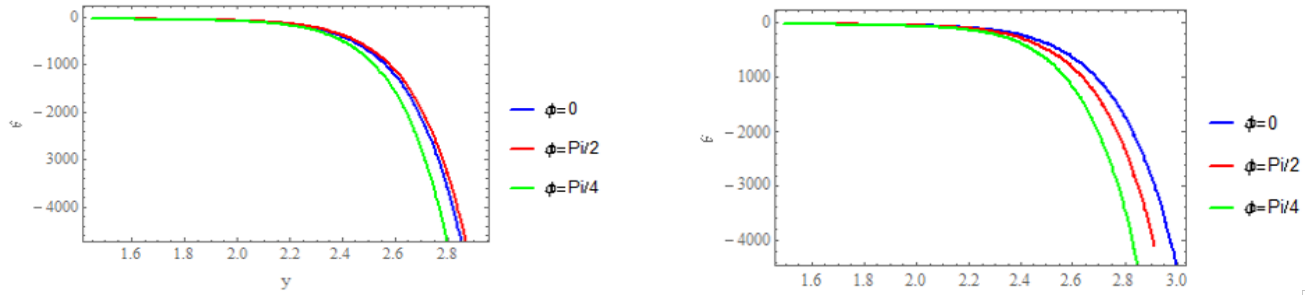

(a) Model-i: Trapezoidal wave (b) Model- ii: Square wave

Figure 8: The variation of Temperature profile (θ) for distinct values of $(\emptyset) at \gamma = 1, M = 1, \beta = 3, a = 0.5, b = 1, \gamma_1 = 0.01, d = 1.8, x = 1.2, \alpha = 3, S_c = 1.5, S_r = 1, P_r = 0.01, D_u = 0.01, D = 0.03.$

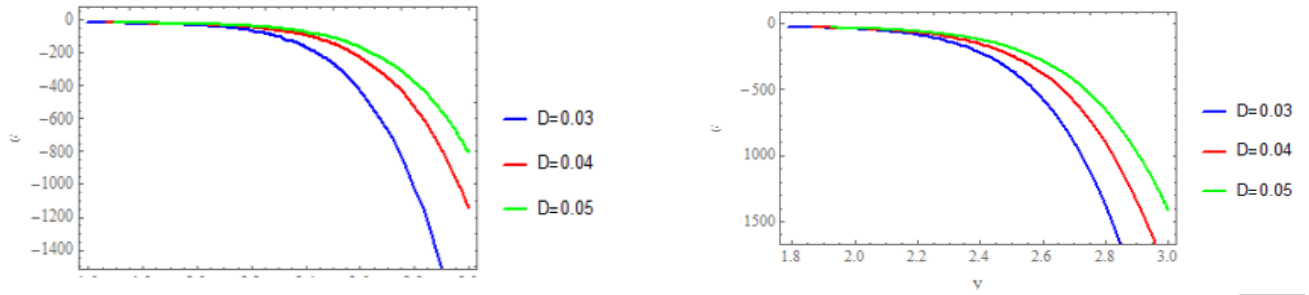

(a) Model-i: Trapezoidal wave (b) Model- ii: Square wave

Figure 9: The variation of Temperature profile (θ) for distinct values of (D) at $\gamma = 1, M = 1, \emptyset = \frac{\pi}{4}, a = 0.5, b = 1, \gamma_1 = 0.01, d = 1.8, x = 1.2, \alpha = 3, S_c = 1.5, S_r = 1, P_r = 0.01, \beta = 9, D_u = 0.01.$

5.3. Concentration profile

Figures (10-14) show the variation of the concentration profile with respect to different parameters. In Figures, it is illustrated that the profile of concentration increases with the increase in chemical reaction parameter (γ_1) at model of trapezoidal wave, While noted reduction in profile at model of square wave as shown in Figure 9. Figure 10 displays the great influence for heat generation parameter (β) between both model. In addition, Figures (11-13) has been drawn to explore the concentration profile against various physical number like Schmidt number (S_c) and Brinkman number (B_r).

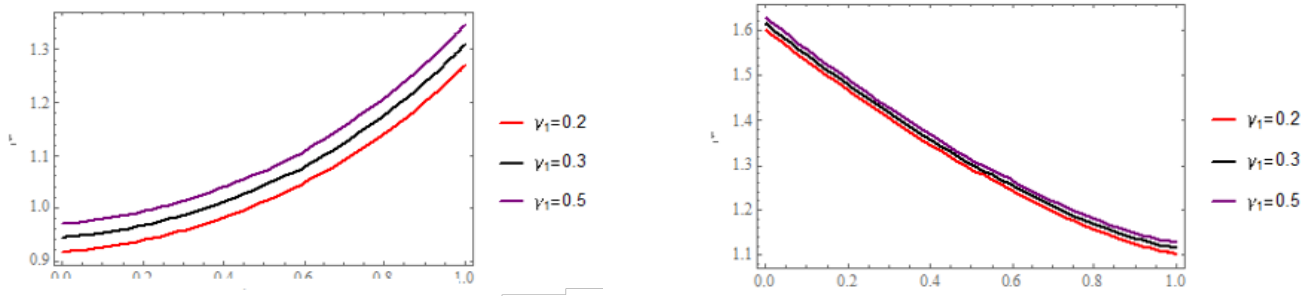

(a) Model-i: Trapezoidal wave (b) Model- ii: Square wave

Figure 10: The variation of Concentration profile (σ) for distinct values of (γ_1) on at $\gamma = 1, M = 1, \emptyset = \frac{\pi}{4}, a = 0.5, b = 1, D = 0.4, d = 1.8, x = 1.2, \alpha = 3, S_c = 1.5, S_r = 1, P_r = 0.1, \beta = 1.3, D_u = 1, B_r = 0.3.$

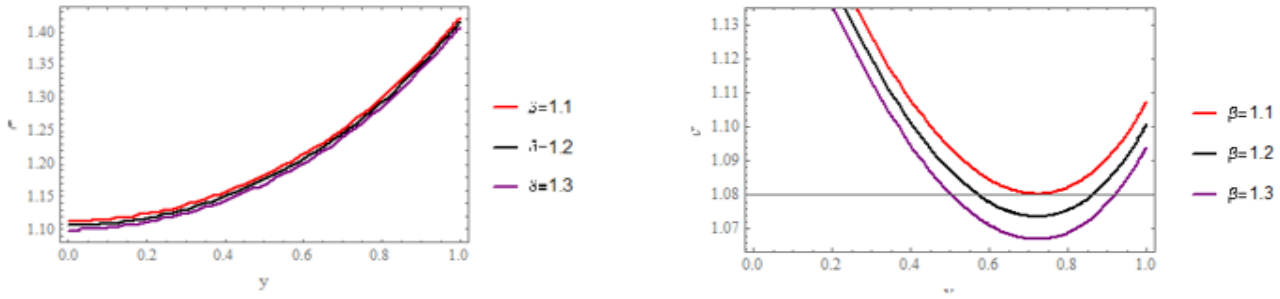

(a) Model-i: Trapezoidal wave (b) Model- ii: Square wave

Figure 11: The variation of Concentration profile (σ) for distinct values (β) at $\gamma = 1, M = 1, \emptyset = \frac{\pi}{4}, a = 0.5, b = 1, D = 0.4, d = 1.8, x = 1.2, \alpha = 3, S_c = 1, S_r = 0.2, P_r = 0.1, \gamma_1 = 0.3, D_u = 1, B_r = 0.3.$

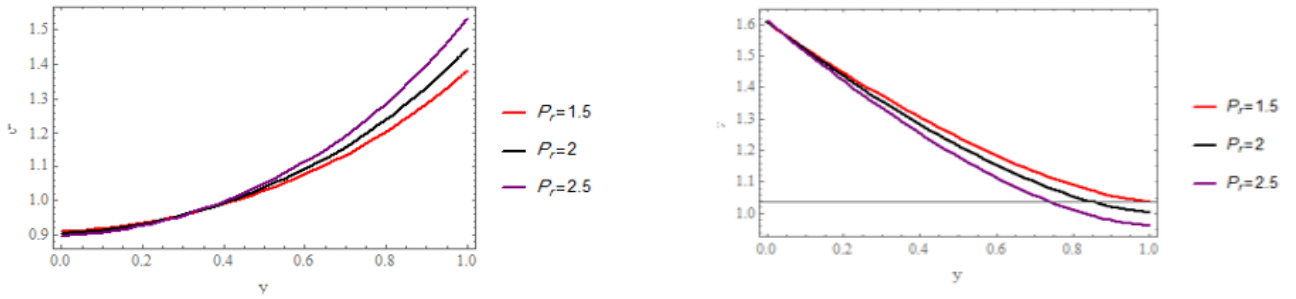

(a) Model-i: Trapezoidal wave (b) Model- ii: Square wave

Figure 12: The variation of Concentration profile (σ) for distinct values (P_r) at $\gamma = 1, M = 1, \emptyset = \frac{\pi}{4}, a = 0.5, b = 1, D = 0.4, d = 1.8, x = 1.2, \alpha = 3, S_c = 1, S_r = 0.2, \beta = 1.3, \gamma_1 = 0.3, D_u = 1, B_r = 0.3.$

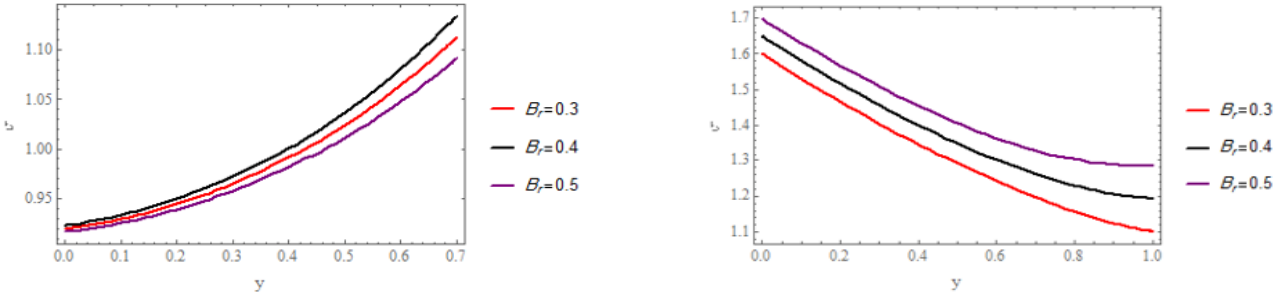

(a) Model-i: Trapezoidal wave (b) Model- ii: Square wave

Figure 13: The variation of Concentration profile (σ) for distinct values (B_r) at $\gamma = 1, M = 1, \emptyset = \frac{\pi}{4}, a = 0.5, b = 1, D = 0.4, d = 1.8, x = 1.2, \alpha = 3, S_c = 1, S_r = 0.2, \beta = 1.3, \gamma_1 = 0.3, D_u = 1, P_r = 0.1.$

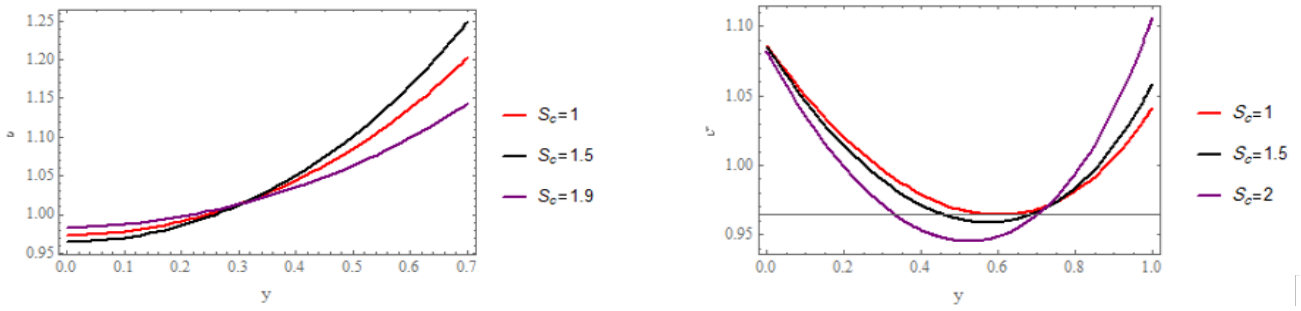

(a) Model-i: Trapezoidal wave (b) Model- ii: Square wave

Figure 14: The variation of Concentration profile (σ) for distinct values (S_c) at $\gamma = 1, \gamma_1 = 0.3, M = 1, \emptyset = \frac{\pi}{4}, a = 0.5, b = 1, D = 0.4, d = 1.8, x = 1.2, \alpha = 3, B_r = 0.3, S_r = 0.2, \beta = 1.3, D_u = 1, P_r = 0.1$.

5.4. Gradient of pressure behavior

Figures (15-18) illustrated variation in pressure gradient with respect to various values of variables such as coefficient of mass diffusivity (D), Froude number (F_r), present couple stress fluid parameter (γ) and (α). According to peristaltic motion, we noticed that oscillatory behavior for $^{dp}/_{dx}$. It can be observed from Figure (13) increasing of value of (D) lead to decrease in pressure gradient as shown in model of trapezoidal wave, While in square wave type divergence and turbulence in waves. In Figures (14) and (15) displayed the impact of increasing in (F_r), (α) increases the pressure gradient. Also, Figure (18) shows the effect of increasing in the value of (γ) at trapezoidal wave with decreases pressure gradually.

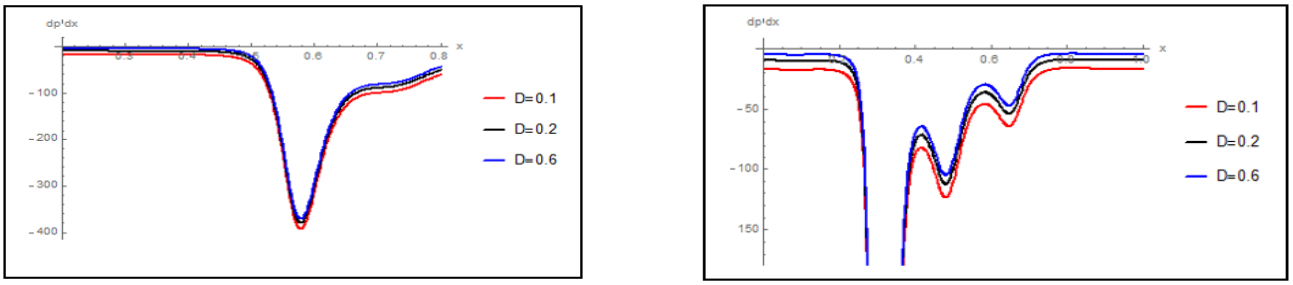

(a) Model-i: Trapezoidal wave (b) Model- ii: Square wave

Figure 15: The variation of Pressure gradient $\left(\frac{dp}{dx}\right)$ for distinct values of (D), at $\gamma = 1, \gamma_1 = 0.3, M = 1, \emptyset = \frac{\pi}{4}, a = 0.5, b = 1, F_r = 0.2, d = 1.8, x = 1.2, \alpha = 3, B_r = 0.3, S_r = 0.2, \beta = 1.3,\ D_u = 1, P_r = 0.1$.

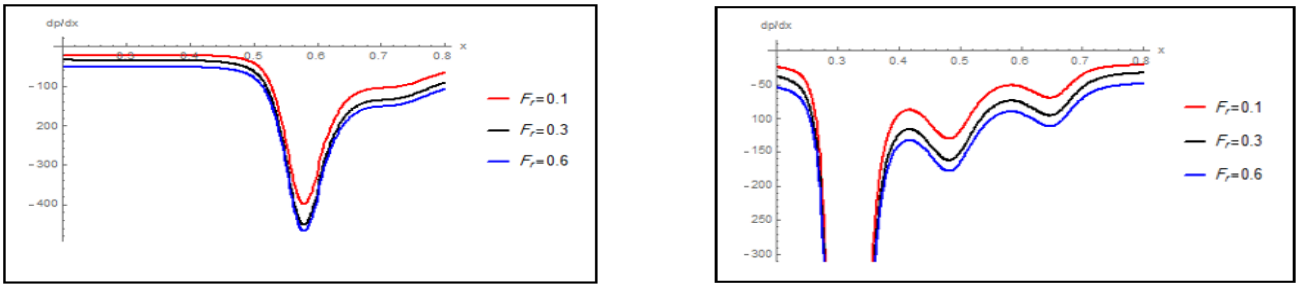

(a) Model-i: Trapezoidal wave (b) Model- ii: Square wave

Figure 16: The variation of Pressure gradient $\left(\frac{dp}{dx}\right)$ for distinct values of (F_r), at $\gamma = 1, \gamma_1 = 0.3, M = 1, \emptyset = \frac{\pi}{4}, a = 0.5, b = 1, D = 0.4, d = 1.8, x = 1.2, \alpha = 3, B_r = 0.3, S_r = 0.2, \beta = 1.3, D_u = 1, P_r = 0.1$.

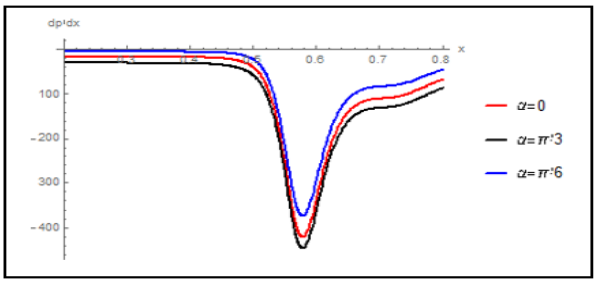

(a) Model-i: Trapezoidal wave

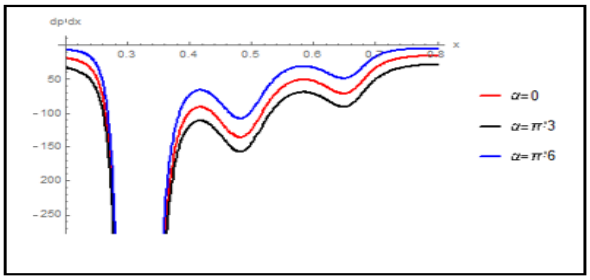

(b) Model- ii: Square wave

Figure 17: The variation of Pressure gradient $\left(\frac{dp}{dx}\right)$ for distinct values of (α), at $\gamma = 1, \gamma_1 = 0.3, M = 1, \emptyset = \frac{\pi}{4}, a = 0.5, b = 1, d = 1.8, D = 0.4, F_r = 0.2, x = 1.2, \alpha = 3, B_r = 0.3, S_r = 0.2, \beta = 1.3, D_u = 1, P_r = 0.1$.

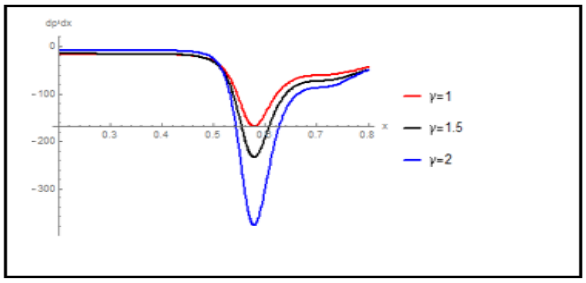

(a) Model-i: Trapezoidal wave

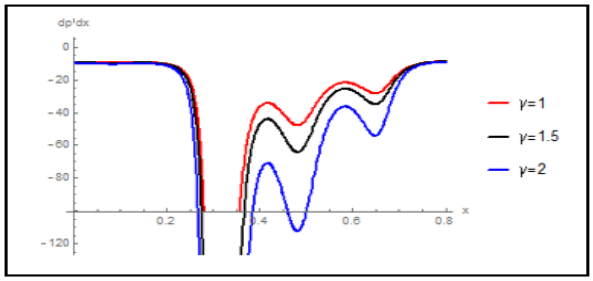

(b) Model- ii: Square wave

Figure 18: The variation of Pressure gradient $\left(\frac{dp}{dx}\right)$ for distinct values of (γ), at $\gamma_1 = 0.3, M = 1, \emptyset = \frac{\pi}{4}, a = 0.5, b = 1, d = 1.8, D = 0.4, x = 1.2, F_r = 0.2, B_r = 0.3, S_r = 0.2, \beta = 1.3, D_u = 1, P_r = 0.1$.

5.5. Trapping phenomena

The closed streamlines of the bolus are formed with respect to the peristaltic motion of the wall of the transport that apply on fluid flow within the channel. In this subsection we will discuss and analyze the impact of some parameters on it. Formation of trapping via the disconnecting of streamlines. On the other hand, streamlines have the same shape as a boundary wall in wave frame. with a view to investigate the influences of trapping phenomenon at various values of γ, D, M. Figures 19 to 24, determine the generation of trapped bolus with variation of physical parameters involved in the stream function (ψ) in the wave frame. In order to investigate the impacts of trapping phenomenon at various boundaries and different values of γ on Figures 19 and 20 were drawn, it is shown that when the value of couple stress fluid parameter (γ) increases, the size of the bolus changes. In Figs.21and 22 illustrate how Hartmann number influence the magnetic force contours. There is a gradually reduction in the size of trapping bolus with increment of of value of (D) as shown in Figures 23 and 24.

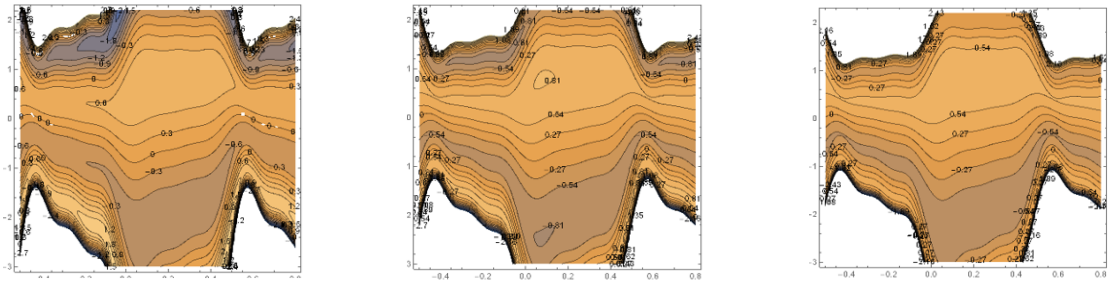

(a) (b) (c)

Figure 19: The effect of (γ) on the streamlines with [trapezoidal wave] at $M = 0.5, \emptyset = \frac{\pi}{6}$, $a = 0.5, b = 1, d = 1.8, D = 0.088, (a)\ \gamma = 1\,(b)\,\gamma = 2\ (c)\,\gamma = 3$.

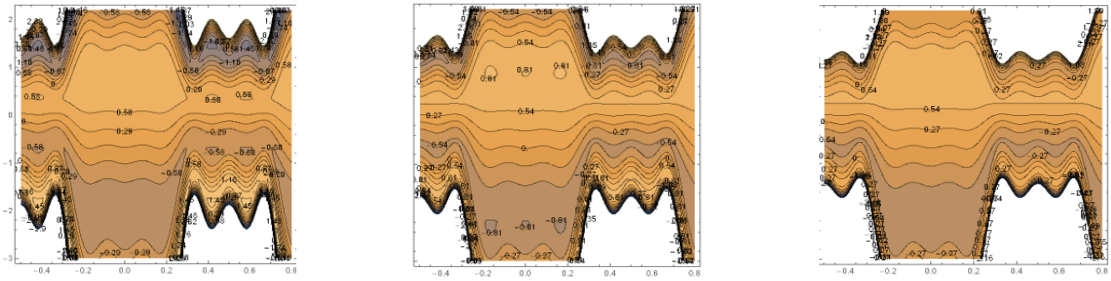

(a) (b) (c)

Figure 20: The effect of (γ) on the streamlines with [square wave] at $M = 0.5, \emptyset = \frac{\pi}{6}, a = 0.5, b = 1, d = 1.8, D = 0.088, \alpha = 3, (a)\,\gamma = 1\,(b)\,\gamma = 2\,(c)\,\gamma = 3$.

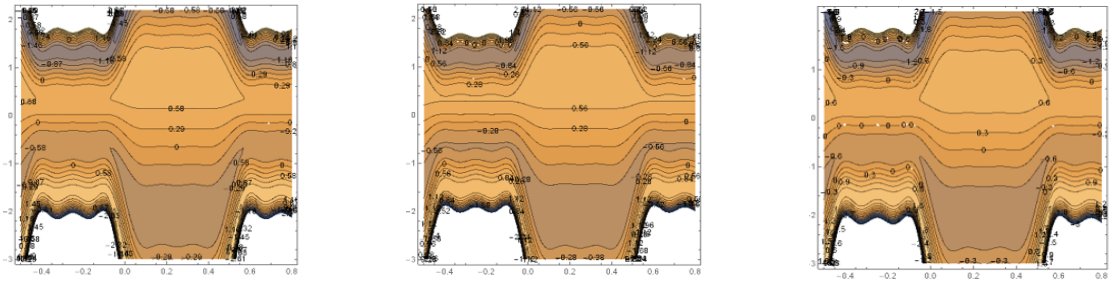

(a) (b) (c)

Figure 21: The effect of (D) on the streamlines with [trapezoidal wave] at $M = 0.5, \emptyset = \frac{\pi}{6}$, $a = 0.5, b = 1, d = 1.8, \gamma = 2, \alpha = 3, (a)\,D = 0.2\,(b)\,D = 0.3\,(c)\,D = 0.5$.

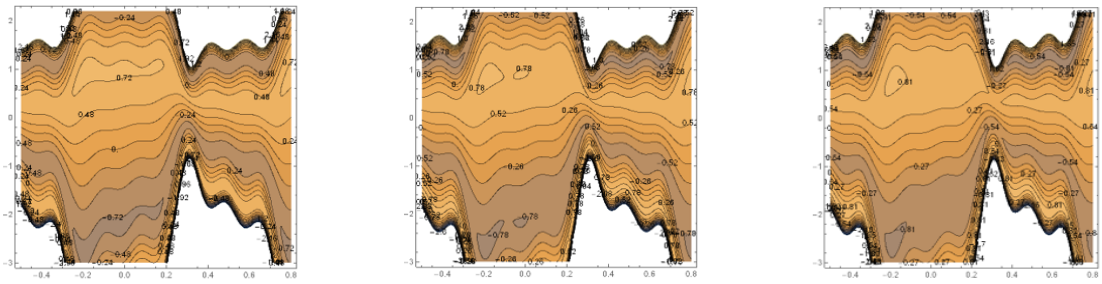

(a) (b) (c)

Figure 22: The effect of (D) on the streamlines with [square wave] at $M = 0.5, \emptyset = \frac{\pi}{6}, a = 0.5, b = 1, d = 1.8, \gamma = 2, \alpha = 3, (a)\ D = 0.2\,(b)\ D = 0.3\,(c)\ \ D = 0.5.$

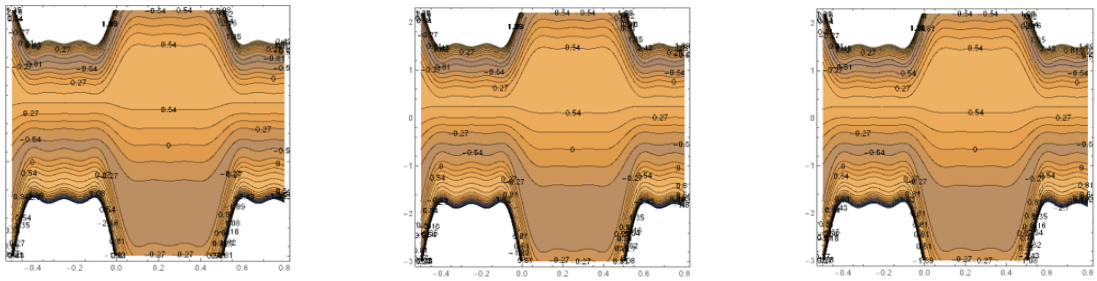

(a) (b) (c)

Figure 23: The effect of (M) on the streamlines with [trapezoidal wave] at $D = 0.088, \emptyset = \frac{\pi}{6}, a = 0.5, b = 1, d = 1.8, \gamma = 2, \alpha = 3, (a)\ M = 0.5\,(b)\ M = 1\,(c)\ \ M = 1.5.$

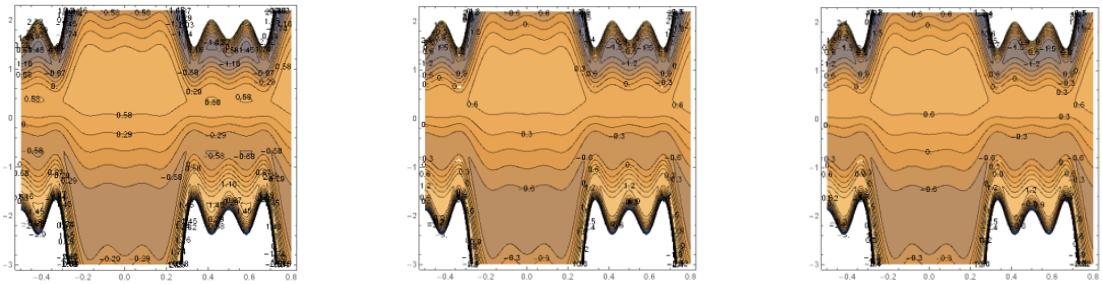

(a) (b) (c)

Figure 24: The effect of (M) on the streamlines with [square wave] at $D = 0.088, \emptyset = \frac{\pi}{6}, a = 0.5, b = 1, d = 1.8, \gamma = 2, \alpha = 3, (a)\ \ M = 0.5\,(b)\ M = 1\,(c)\ \ M = 1.5.$

6. Conclusion

The current study is performed to analyze and explain the peristaltic transport of couple stress fluid with variable viscosity and chemical reaction. Non-linear equations are simplified via considering long wavelength and small Reynolds number approximation. Due to the exhibited analysis, following outcomes observations are the main of this study.

1. Note that, the axial velocity distribution is parabolic path and increase near middle of channel. But, at walls of part og the channel we observe the velocity increases due to increasing amount of variables at both model trapezoidal and square wave.

2. It can be seen that, The temperature felid diminishes upon decreasing almost parameters and decreasing with others and (θ) temperature versus y-axis as shown in Figs.
3. For instance, concentration profile as we announced that larger values of heat generation parameter (β) and effects of Schmidt number (S_c) have enormous weight, specifically in case of square waves model.
4. Pressure gradient diverges and increases with Froude number as well as the amount of (α) on channel.
5. Generally, in the phenomenon of trapping that observes peristaltic flow of couple stress fluid under certain conditions ,Which compare between two points for trapezoidal waveform and square waveform.
6. When the values of "M" and "D" a"e increased, the trapped bolus are eliminated.
7. Both of waveforms and different boundaries exhibited various impacts on every distribution of this manuscript, Which makes us in future head to extended, generalized this work.

References

[1] S. Nadeem, N. S. Akbar, Peristaltic flow of a jeffrey fluid with variable viscosity in an asymmetric channel, Zeitschrift für Naturforschung A 64 (11) (2009) 713–722.

[2] R. Latha, B. R. Kumar, O. D. Makinde, Peristaltic flow of couple stress fluid in an asymmetric channel with partial slip, Defect and Diffusion Forum 387 (2018) 385–402.

[3] A. Alsaedi, N. Ali, D. Tripathi, T. Hayat, Peristaltic flow of couple stress fluid through uniform porous medium, Applied Mathematics and Mechanics 35 (2014) 469–480.

[4] A. Afsar Khan, R. Ellahi, K. Vafai, et al., Peristaltic transport of a jeffrey fluid with variable viscosity through a porous medium in an asymmetric channel, Advances in Mathematical Physics 2012 (2012).

[5] S. Nadeem, N. S. Akbar, Effects of heat transfer on the peristaltic transport of mhd newtonian fluid with variable viscosity: application of adomian decomposition method, Communications in Nonlinear Science and Numerical Simulation 14 (11) (2009) 3844–3855.

[6] R. S. Kareem, A. M. Abdulhadi, Impacts of heat and mass transfer on magneto hydrodynamic peristaltic flow having temperature-dependent properties in an inclined channel through porous media, Iraqi Journal of Science 61 (4) (2020) 854–869.

[7] A. Bhattacharyya, R. Kumar, G. Seth, Capturing the features of peristaltic transport of a chemically reacting couple stress fluid through an inclined asymmetric channel with dufour and soret effects in presence of inclined magnetic field, Indian Journal of Physics 95 (2021) 2741–2758.

[8] S. Farooq, M. I. Khan, T. Hayat, M. Waqas, A. Alsaedi, Theoretical investigation of peristalsis transport in flow of hyperbolic tangent fluid with slip effects and chemical reaction, Journal of Molecular Liquids 285 (2019) 314–322.

[9] R. Muthuraj, K. Nirmala, S. Srinivas, Influences of chemical reaction and wall properties on mhd peristaltic transport of a dusty fluid with heat and mass transfer, Alexandria Engineering Journal 55 (1) (2016) 597–611.

[10] M. Rafiq, M. Sajid, S. E. Alhazmi, M. I. Khan, E. R. El-Zahar, Mhd electroosmotic peristaltic flow of jeffrey nanofluid with slip conditions and chemical reaction, Alexandria Engineering Journal 61 (12) (2022) 9977–9992.

[11] G. S. Seth, A. Bhattacharyya, R. Kumar, M. K. Mishra, Modeling and numerical simulation of hydromagnetic natural convection casson fluid flow with nth-order chemical reaction and newtonian heating in porous medium, Journal of porous Media 22 (9) (2019) 1141–1157.

[12] Q. K. Jawad, A. M. Abdulhadi, Influence of mhd and porous media on peristaltic transport for nanofluids in an asymmetric channel for different types of walls, International Journal of Nonlinear Analysis and Applications 14 (1) (2023) 819–832.

[13] S. A. Abdulla, L. Z. Hummady a, Inclined magnetic field and heat transfer of asymmetric and porous medium channel on hyperbolic tangent peristaltic flow, International Journal of Nonlinear Analysis and Applications 12 (2) (2021) 2359–2372.

[14] A. W. Salih, S. B. Habeeb, Peristaltic flow with nanofluid under effects of heat source, and inclined magnetic field in the tapered asymmetric channel through a porous medium, Iraqi Journal of Science 63 (10) (2022) 4445–4459.

[15] A. M. Nassief, A. M. Abdulhadi, Influence of magnetic force for peristaltic transport of non-newtonian fluid through porous medium in asymmetric channel, Iraqi Journal of Science 64 (7) (2023) 4467–4486.

[16] M. Khader, Numerical solutions for the problem of the boundary layer flow of a powell–eyring fluid over an exponential sheet using the spectral relaxation method, Indian Journal of Physics 94 (2020) 1369–1374.

[17] K. Ramesh, Influence of heat and mass transfer on peristaltic flow of a couple stress fluid through porous medium in the presence of inclined magnetic field in an inclined asymmetric channel, Journal of Molecular Liquids 219 (2016) 256–271.

[18] G. G. Mohammed, A. W. Salih, et al., Impacts of porous medium on unsteady helical flows of generalized oldroyd-b fluid with two infinite coaxial circular cylinders, Iraqi Journal of Science 62 (5) (2021) 1686–1694.

[19] M. R. Salman, A. M. Abdulhadi, Influence of heat and mass transfer on inclined (mhd) peristaltic of pseudoplastic nanofluid through the porous medium with couple stress in an inclined asymmetric channel, Journal of Physics: Conference Series 1032 (1) (2018) 012043.

[20] R. Y. Hassen, H. A. Ali, Hall and joule's heating influences on peristaltic transport of bingham plastic fluid with variable viscosity in an inclined tapered asymmetric channel, Ibn AL-Haitham Journal For Pure and Applied Sciences 34 (1) (2021) 68–84.

[21] J. Prakash, E. Siva, A. Govindarajan, M. Vidhya, Influence of variable viscosity on peristaltic motion of a viscoelastic fluid in a tapered micro fluidic vessel, International Journal of Engineering & Technology 7 (4.10) (2018) 49–54.
[22] A. W. Salih, et al., Influence of rotation, variable viscosity and temperature on peristaltic transport in an asymmetric channel, Turkish Journal of Computer and Mathematics Education (TURCOMAT) 12 (6) (2021) 1047–1059.
[23] S. Akram, N. Saleem, et al., Analysis of heating effects and different wave forms on peristaltic flow of carreau fluid in rectangular duct, Advances in Mathematical Physics 2020 (2020).
[24] Z. A. Jaafar, L. Z. Hummady, M. H. Thawi, Influence of some fluid mechanic parameters caused from heat transport with rotation on walter's b fluid, Journal of Biomechanical Science and Engineering (2023) 20–32.
[25] H. A. Ali, Radiative peristaltic transport of ree-eyring fluid through porous medium in asymmetric channel subjected to combined effect of inclined mhd and convective conditions, Journal of Physics: Conference Series 1879 (2) (2021) 022101.
[26] R. S. Kareem, A. M. Abdulhadi, Effect of mhd and porous media on nanofluid flow with heat transfer: Numerical treatment, Journal of advanced research in fluid mechanics and thermal sciences 63 (2) (2019) 317–328.
[27] N. T. Eldabe, K. A. Kamel, S. F. Ramadan, R. A. Saad, Peristaltic motion of eyring-powell nano fluid with couple stresses and heat and mass transfer through a porous media under the effect of magnetic field inside asymmetric vertical channel, Journal of Advanced Research in Fluid Mechanics and Thermal Sciences 68 (2) (2020) 58–71.
[28] L. Z. Hummady, et al., Effect of couple stress on peristaltic transport of powell-eyring fluid peristaltic flow in inclined asymmetric channel with porous medium, Wasit Journal of Computer and Mathematics Sciences 1 (2) (2022) 106–118.
[29] H. Abdulhussein, A. M. Abdulhadi, Impact of couple stress and rotation on peristaltic transport of a powell-eyring fluid in an inclined asymmetric channel with hall and joule heating, journal of Basic Sciences 8 (13) (2022).
[30] M. Dhlamini, H. Mondal, P. Sibanda, S. Motsa, Numerical analysis of couple stress nanofluid in temperature dependent viscosity and thermal conductivity, International Journal of Applied and Computational Mathematics 7 (2021) 1–14.
[31] S. Manjunatha, B. Gireesha, Effects of variable viscosity and thermal conductivity on mhd flow and heat transfer of a dusty fluid, Ain Shams Engineering Journal 7 (1) (2016) 505–515.
[32] T. Kannan, M. Moorthy, Effects of variable viscosity on power-law fluids over a permeable moving surface with slip velocity in the presence of heat generation and suction, Journal of Applied Fluid Mechanics 9 (6) (2016) 2791–2801.
[33] F. Abbasi, T. Hayat, B. Ahmad, Hydromagnetic peristaltic transport of variable viscosity fluid with heat transfer and porous medium, J. Applied Mathematics and Information Sciences 10 (6) (2016) 2173–2181.
[34] O. Makinde, T. Iskander, F. Mabood, W. Khan, M. Tshehla, Mhd couette-poiseuille flow of variable viscosity nanofluids in a rotating permeable channel with hall effects, Journal of Molecular liquids 221 (2016) 778–787.
[35] B. Tripathi, B. K. Sharma, Effect of variable viscosity on mhd inclined arterial blood flow with chemical reaction, International Journal of Applied Mechanics and Engineering 23 (3) (2018) 767–785.
[36] A. Hakeem, M. Nayak, O. Makinde, Effect of exponentially variable viscosity and permeability on blasius flow of carreau nano fluid over an electromagnetic plate through a porous medium, Journal of Applied and Computational Mechanics 5 (2) (2019) 390–401.
[37] J. Falade, S. Adesanya, J. Ukaegbu, M. Osinowo, Entropy generation analysis for variable viscous couple stress fluid flow through a channel with non-uniform wall temperature, Alexandria Engineering Journal 55 (1) (2016) 69–75.
[38] A. Khan, M. Farooq, R. Nawaz, M. Ayaz, H. Ahmad, H. Abu-Zinadah, Y.-M. Chu, Analysis of couple stress fluid flow with variable viscosity using two homotopy-based methods, Open Physics 19 (1) (2021) 134–145.
[39] A. Disu, M. Dada, Reynold's model viscosity on radiative mhd flow in a porous medium between two vertical wavy walls, Journal of Taibah University for Science 11 (4) (2017) 548–565.
[40] S. K. Mondal, D. Pal, Computational analysis of bioconvective flow of nanofluid containing gyrotactic microorganisms over a nonlinear stretching sheet with variable viscosity using ham, Journal of Computational Design and Engineering 7 (2) (2020) 251–267.
[41] P. Hariharan, V. Seshadri, R. K. Banerjee, Peristaltic transport of non-newtonian fluid in a diverging tube with different wave forms, Mathematical and Computer Modelling 48 (7-8) (2008) 998–1017.
[42] S. Nadeem, S. Akram, Peristaltic flow of a maxwell model through porous boundaries in a porous medium, Transport in Porous Media 86 (2011) 895–909.
[43] F. A. Adnan, A. M. A. Hadi, Effect of an inclined magnetic field on peristaltic flow of bingham plastic fluid in an inclined symmetric channel with slip conditions, Iraqi Journal of Science 60 (7) (2019) 1551–1574.
[44] D. Lu, A. Seadawy, M. Arshad, Applications of extended simple equation method on unstable nonlinear schrödinger equations, Optik 140 (2017) 136–144.
[45] S. Akram, S. Nadeem, Influence of nanoparticles phenomena on the peristaltic flow of pseudoplastic fluid in an inclined asymmetric channel with different wave forms, Iranian Journal of Chemistry and Chemical Engineering 36 (2) (2017) 107–124.
[46] G. Shit, S. Majee, Magnetic field interaction with blood flow and heat transfer through diseased artery having abdominal aortic aneurysm, European Journal of Mechanics-B/Fluids 71 (2018) 1–14.
[47] V. Narla, D. Tripathi, O. A. Bég, Analysis of entropy generation in biomimetic electro osmotic nanofluid pumping through a curved channel with joule dissipation, Thermal Science and Engineering Progress 15 (2020) 100424.
[48] A. Riaz, H. Alolaiyan, A. Razaq, Convective heat transfer and magneto hydrodynamics across a peristaltic channel coated with nonlinear nanofluid, Coatings 9 (12) (2019) 816.
[49] S. Akram, N. Saleem, et al., Analysis of heating effects and different wave forms on peristaltic flow of carreau fluid in rectangular duct, Advances in Mathematical Physics 2020 (2020).

[50] S. Akram, M. Athar, K. Saeed, A. Razia, M. Alghamdi, T. Muhammad, Impact of partial slip on double diffusion convection of sisko nanofluids in asymmetric channel with peristaltic propulsion and inclined magnetic field, Nanomaterials 12 (16) (2022) 2736.